Full paper

Applied Organometallic Chemistry

Received: 16 December 2015 Revised: 6 January 2016 Accepted: 10 January 2016 Published online in Wiley Online Library: 10 March 2016

(wileyonlinelibrary.com) DOI 10.1002/aoc.3448

Design, preparation and characterization of Cu/GA/Fe_3O_4@SiO_2 nanoparticles as a catalyst for the synthesis of benzodiazepines and imidazoles

Ahmad Shaabani*, Heshmatollah Sepahvand, Seyyed Emad Hooshmand and Mahmoud Borjian Boroujeni

The synthesis and characterization of an efficient and reusable nanocatalyst, Cu/GA/Fe_3O_4@SiO_2, obtained by ultrasonic-assisted grafting of guanidineacetic acid on modified Fe_3O_4@SiO_2 core–shell nanocomposite spheres and subsequent immobilization of Cu (II), are described. The catalyst was characterized by means of X-ray diffraction, scanning and transmission electron microscopies, energy-dispersive X-ray spectroscopy, elemental analysis, thermogravimetric analysis, Fourier transform infrared spectroscopy, vibrating sample magnetometry and inductively coupled plasma optical emission spectrometry. The prepared nanocatalyst facilitated an efficient and straightforward friendly procedure for the synthesis of benzodiazepines and imidazoles in ethanol and under solvent-free conditions, respectively. The nanocatalyst can be easily recovered using a magnet and reused several times without any significant loss of activity. Copyright © 2016 John Wiley & Sons, Ltd.

Keywords: Cu(II) nanocatalyst; ultrasonic-assisted; benzodiazepine; imidazole; magnetically recoverable

Introduction

Nanoscience is one of the most important research and development frontiers in modern science.[1] Owing to the unique size and physical properties of nanomaterials, it is desirable among researchers to use spherical nanoparticles for biomedical applications, including enzyme encapsulation, DNA transfection, biosensors and catalytic applications.[2,3] In particular, surface-functionalized mesoporous silica materials and supported magnetic metal nanoparticles such as mesoporous silica-supported Fe_3O_4 nanoparticles have been increasingly used as heterogeneous catalysts in the synthesis of organic and medicinal compounds.[4,5] Numerous strategies have been described for immobilizing inorganic and/or organic active species on or within silica matrices. Functionalization of mesoporous silica surface via connecting to active groups can generally be done using two methods: (i) post-modification method, which involves grafting an organotrialkoxysilane onto the pore surfaces after mesoporous material synthesis and (ii) direct modification method, in which the functional groups are introduced during the synthesis of the mesoporous materials. Pore functionalization is achieved through the co-condensation reaction occurring between the organotrialkoxysilane and the silica source in the presence of a structure-directing agent.[6] The direct synthesis method is considered more predictable and hence valuable, because it can avoid several shortcomings of the post-grafting method, such as reduction in pore size, pore blocking at the aperture and difficulties in controlling the loadings as well as the distribution of active sites.[7] An important feature of these catalysts is their simple separation using an external magnet without filtration. Furthermore, functionalized Fe_3O_4@SiO_2 catalysts show not only high catalytic activity but also a high degree of chemical stability in various organic solvents. Also, these catalysts show high thermal stability and maintain their activity.[4] These properties combined with the high accessibility of the globular arranged active sites of certain surface-modified Fe_3O_4@SiO_2 nanoparticles have encouraged their applications as supports for palladium and chiral ruthenium complexes, or organocatalysts such as 4-*N*,*N*-dimethylaminopyridine or proline.[8]

Multicomponent reactions (MCRs) are powerful tools for the total synthesis of natural products,[9] design and discovery of biologically active molecules[10] and various heterocyclic compounds[11,12] from simple and readily accessible starting materials. The atom economy of MCRs, their convergent character, operational simplicity and the structural diversity and complexity of the resulting molecules make this chemistry exceptionally useful for discovery and optimization processes in the pharmaceutical industry.[13] In the presence of a catalyst, MCRs are fast and more selective methods for the synthesis of large libraries of organic molecules with the widest range of each component.[14] Benzodiazepine and imidazole scaffolds are two great examples of these organic molecules which have been synthesized through diverse ways in recent years. Recently, some strategies have been introduced for the synthesis of substituted benzodiazepines. These methods are based on condensation of *o*-phenylenediamine and aldehydes with various cyclic or acyclic ketones in the presence

* *Correspondence to: Ahmad Shaabani, Shahid Beheshti University, Faculty of Chemistry, PO Box 19396-4716, Tehran, Islamic Republic of Iran. E-mail: a-shaabani@sbu.ac.ir*

Faculty of Chemistry, Shahid Beheshti University, PO Box 19396-4716Tehran, Islamic Republic of Iran

of a wide variety of heterogeneous and homogeneous catalysts such as $Yb(OTf)_3$,[15] SiO_2,[16] polyfluorinated zinc(II) phthalocyanine complex[17] and Fe_3O_4@chitosan.[18] The synthesis of highly substituted imidazoles has been performed by condensation of benzil and benzoin, aldehydes and ammonium acetate in the presence of silica sulfonic acid,[19] $ZrCl_4$,[20] Al_2O_3,[21] tetrabutylammonium bromide,[22] nanocrystalline magnesium oxide[23] and inorganic acid.[[24–26]] However, most of these methods have some disadvantages including moderate yields, harsh reaction conditions, long reaction times and use of microwave irradiation.

In continuation of our work towards the synthesis of benzodiazepine and imidazole derivatives as well as our interest in the preparation and use of heterogeneous catalysts in organic synthesis,[27–29] we synthesized and characterized magnetically recoverable nanocomposite particles (NCPs), Cu/GA/Fe_3O_4@SiO_2, and investigated their activity as nanocatalyst in the synthesis of substituted benzodiazepines and 2,4,5-trisubstituted imidazoles. The corresponding reactions are shown in Scheme 1.

Experimental

Materials

Tetraethoxysilane (TEOS; 99%), chloropropyltriethoxysilane (CPTES; 99%), guanidineacetic acid (GA) and absolute ethanol (EtOH; 99%) were purchased from Merck and used without further purification.

Instrumentation

Fourier transform infrared (FT-IR) spectra were recorded using a Bomem MB-Series FT-IR spectrophotometer. Morphological measurements were performed using a transition electron microscopy (TEM) instrument (Philips CM10) operated at an 80 kV electron beam accelerating voltage. Scanning electron microscopy (SEM) and energy-dispersive X-ray spectroscopy (EDX) were performed with a Philips XL-300 instrument. The sample was sputtered with gold to avoid undesirable electron charging. X-ray diffraction (XRD) was conducted using a Philips X'pert Pro (PW 3040) X-ray diffractometer with monochromatic Cu Kα radiation (1.54056 Å, 40 kV, 30 mA). Thermogravimetric analysis (TGA) was conducted using a TG/DTA6300 instrument, at a heating rate of 20°C min^{-1} under nitrogen flow. Elemental analysis was performed with a CHN machine (PerkinElmer Series II, 2400). ^{1}H NMR spectra were recorded with a Bruker DRX-400 spectrometer at 300 MHz. The concentration of copper was estimated using a Shimadzu AA-680 flame atomic absorption spectrophotometer and an inductively coupled plasma optical emission spectrometer (ICP-OES; Varian Vista PRO Radial). The magnetic properties of particles were analysed using vibrating sample magnetometry (Meghnatis Daghigh Kavir Co., Iran) equipment (I_{max} = 150 A, $P \leq 9$ kW) at room temperature.

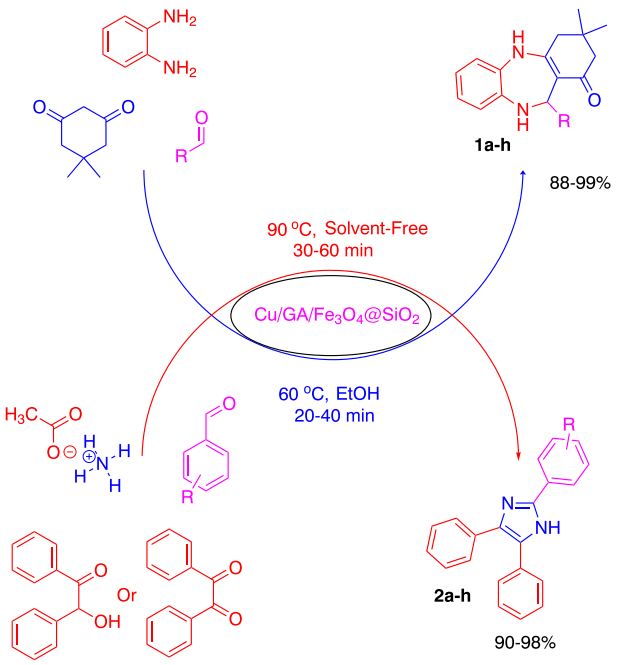

Scheme 1. Cu/GA/Fe_3O_4@SiO_2-catalyzed synthesis of substituted benzodiazepines and imidazoles.

Preparation of modified Fe_3O_4@SiO_2 NCPs

$FeCl_3 \cdot 6H_2O$ (1.00 g, 3.70 mmol) and $FeCl_2 \cdot 4H_2O$ (0.37 g, 1.80 mmol) were dissolved in 20 ml of deionized water under nitrogen gas with vigorous stirring. Then, NH_3 (25%) was added into the solution until the pH reached 10. Stirring was continued for 1 h at 60°C. The colour of the bulk solution turned from orange to black immediately. The magnetite precipitate was separated from the solution using a magnet, washed several times with deionized water and EtOH, and left to dry in air. Then, 30 mg of the as-synthesized Fe_3O_4 nanoparticles was mixed with 50 ml of isopropyl alcohol in a sealed three-neck flask using ultrasonic treatment for 30 min. Amounts of 10 ml of deionized water, 0.15 ml of TEOS (silica precursor) and 1.70 ml of NH_3 (25%) were added into the mixture of Fe_3O_4 and isopropyl alcohol at ambient temperature under mechanical agitation. After 12 h, the product, Fe_3O_4@SiO_2, was collected, washed with EtOH and deionized water and dried at 50°C. The silica-coated Fe_3O_4 nanoparticles were functionalized using a post-modification method with CPTES by refluxing in anhydrous toluene at 110°C for 24 h (modified Fe_3O_4@SiO_2).

Immobilization of GA on the surface of modified Fe_3O_4@SiO_2 NCPs

GA (5.00 g, 4.27 mmol) was added into a suspension of modified Fe_3O_4@SiO_2 powder (1.00 g) in water (30 ml). The reaction mixture was sonicated at 60°C in an ultrasonic bath for 1 h. The solid phase was separated using an external magnet and washed with EtOH. Finally, the solid sample was dried at 100°C for 24 h (GA/Fe_3O_4@SiO_2).

Chelation of Cu(II) on the surface of GA/Fe_3O_4@SiO_2 NCPs

The as-synthesized GA/Fe_3O_4@SiO_2 NCPs (1.00 g) were dispersed in 10 ml of deionized water solution containing copper(II) chloride dehydrate (0.17 g, 1.00 mmol). The reaction mixture was stirred for 12 h. Then, the solid phase was filtered by applying an external magnet and washed two times with deionized water. It was dried at 100°C for 12 h (Cu/GA/Fe_3O_4@SiO_2). The loading of copper was obtained as 0.72 mmol g^{-1} as measured using ICP-OES.

Preparation of Cu(II)-supported [*N*′-(3-triethoxysilanepropyl) guanidino]acetic acid

A mixture of GA (0.12 g, 1.00 mmol) and CPTES (0.24 g, 1.00 mmol) in deionized water was sonicated at 60°C for 1 h. After completion of reaction, the reaction mixture was collected and washed (2 × 5 ml) with a solution of $NaHCO_3$ (0.1 M) to afford a brown powder.

Yield 0.31 g; m.p. > 300°C. Anal. Calcd for $C_{12}H_{27}N_3O_5Si$ (%): C, 44.84; H, 8.47; N, 13.07. Found (%): C, 43.97; H, 9.01; N, 12.98. FT-IR (KBr, cm^{-1}): 3389, 3303, 2972, 2867, 1678, 1627, 1586, 1405, 1375, 1145. ^{1}H NMR (300 MHz, $CDCl_3$, δ, ppm): 8.08 (1 H, s, NH), 4.97 (2 H, s, NH_2), 4.19 (2 H, s, CH_2COOH), 3.53 (6 H, q, $^3J_{HH}$ = 5.3 Hz, CH_3CH_2–OSi), 3.12 (2 H, t, $^3J_{HH}$ = 5.4 Hz, $CH_2CH_2CH_2$NH), 1.54 (2 H, m, $CH_2CH_2CH_2$NH), 1.24 (9 H, t, ^3J = 5.3 Hz, CH_3CH_2–OSi), 0.47 (2 H, t, ^3J = 5.4 Hz, $CH_2CH_2CH_2$NH). ^{13}C NMR (75 MHz, $CDCl_3$, δ, ppm): 12.7 ($SiCH_2$–), 19.1 (CH_3), 26.8 ($SiCH_2CH_2$), 40.2 (–CH_2CH_2NH), 42.5 (CH_2COOH), 56.9 (CH_3CH_2O), 156.2 ($NCNH_2$), 179.8 (C=O).

The [*N*′-(3-triethoxysilanepropyl)guanidino]acetic acid was added to solution of copper(II) chloride dehydrate (0.17 g, 1.00 mmol) in deionized water. The reaction mixture was stirred for 12 h at room temperature. Subsequently, the reaction mixture was separated using an external magnet and washed with deionized water (2 × 5 ml). Finally, the obtained solid was dried at 100°C for 12 h (Cu/GA/CPTES). Anal. Calcd for $C_{24}H_{52}CuN_6O_{10}Si_2$ (%): C, 40.92; H, 7.44; N, 11.93. Found (%): C, 41.84; H, 7.92; N, 13.43. The content of the copper was 1.48 mmol g^{-1} as measured using ICP-OES.

General procedure for synthesis of benzodiazepine derivatives in presence of Cu/GA/Fe_3O_4@SiO_2 NCPs

To a mixture of a *o*-phenylenediamine (**1**) (0.11 g, 1 mmol) and dimedone (**2**) (0.14 g, 1 mmol) in EtOH (5 ml) was added Cu/GA/Fe_3O_4@SiO_2 (0.01 g, 0.72 mol%), and the mixture was stirred at room temperature for 5–10 min to give an intermediate product. After confirmation of the formation of the intermediate using TLC (EtOAc–*n*-hexane, 2:1), an aldehyde (**3**) (1 mmol) was added and the reaction was continued for 15–30 min at 60°C. After completion, as indicated by TLC (EtOAc–*n*-hexane, 3:1), the catalyst was separated from the mixture using an external magnet, and the solvent was evaporated. Finally, the product was recrystallized from EtOH–water (1:1) to afford pure benzodiazepine.

3,3-Dimethyl-11-*p*-tolyl-2,3,4,5,10,11-hexahydrodibenzo[*b*, *e*][1,4]diazepin-1-one (**1f**). Green powder. FT-IR (KBr, cm^{-1}): 3327, 3265, 3043, 2962, 1595, 1382, 1530, 1317, 1461. ^{1}H NMR (300 MHz, DMSO, δ, ppm): 1.01(3 H, s, CH_3), 1.09 (3 H, s, CH_3), 2.01 (2 H, ABq, *J* = 16 Hz, CH_2), 2.08 (3 H, s, CH_3–Ar), 2.59 (2 H, s, –CH_2–C=O), 5.69 (1 H, s, N–H), 5.89 (1 H, s, CH), 6.23–6.93 (8 H, m, ArH), 8.55 (1 H, s, N–H). ^{13}C NMR (75 MHz, DMSO, δ, ppm): 21.8 (CH_3–Ar), 29.1 (CH_3), 32.4 ((CH_3)$_2$*C*(CH_2)$_2$), 45.0 (CH_2C), 50.1 (CH_2CO), 54.6 (CH), 111.6 (*C*CO), 119.8, 120.2, 121.1, 122.9, 126.2, 127.5, 127.9, 131.5, 138.1, 145.1, 155.1 (C–Ar and CH_2CNH), 192.5 (C=O).

Typical procedure for synthesis of 2-(4-methylphenyl)-4,5-diphenylimidazole in presence of Cu/GA/Fe_3O_4@SiO_2 NCPs

A mixture of 4-methylbenzaldehyde (0.12 g, 1 mmol), benzil or benzoin (1 mmol), ammonium acetate (0.30 g, 4 mmol) and Cu/GA/Fe_3O_4@SiO_2 (0.01 g, 0.72 mol%) was heated at 90°C for 30 min under solvent-free conditions. The solid residue was washed with acetone and the solvent was evaporated to give the crude product. For further purification, it was recrystallized from 9:1 acetone–water mixture to afford pure product **2d** as a colourless powder.

FT-IR (KBr, cm^{-1}): 1441, 1495, 1610, 3023. ^{1}H NMR (300 MHz, $CDCl_3$, δ, ppm): 2.30 (3 H, s, CH_3), 7.26–7.64 (12 H, m, Ar), 7.71 (2 H, d, *J* = 8 Hz, Ar), 9.60 (1 H, s, NH). ^{13}C NMR (75 MHz, $CDCl_3$, δ, ppm): 21.8 (CH_3–Ar), 124.7, 127.4, 128.8, 128.9, 129.2, 129.6, 129.8, 130.0, 139.2 (C–Ar), 146.6 (–NCNH).

Results and discussion

Preparation and characterization of catalyst

The Cu/GA/Fe_3O_4@SiO_2 nanocatalyst was prepared with a multi-step reaction. Initially, iron oxide NCPs as a magnetic core were coated with a silica layer via a sol–gel method in isopropyl alcohol. For immobilization of the organic catalyst on the surface of the inorganic support, first, the surface was modified using an appropriate coupling agent to make covalent bonds with the active species. It is known that organosilanes can act as a linker between the organic species and the support.[30] Next, some of the linker's chloride was replaced by nitrogen of GA via a S_N2 reaction. The GA was anchored onto the surface of modified-SiO_2/Fe_3O_4 to obtain the bifunctional modified magnetic NCPs of GA/Fe_3O_4@SiO_2. A procedure for the synthesis of GA/Fe_3O_4@SiO_2 was carried out using an ultrasonic-assisted method which involved grafting GA onto surface of modified NCPs in aqueous medium. Subsequently, GA/Fe_3O_4@SiO_2 was added to aqueous $CuCl_2$ solution to afford the supported Cu catalyst (Cu/GA/Fe_3O_4@SiO_2) (Scheme 2, pathway 1). To ensure the presence of new functional groups, each step of the catalyst preparation procedure was monitored using FT-IR, TGA and CHN. It is possible to attach both amine groups of GA to the surface. To clarify how GA moieties are connected to the surface of modified NCPs, GA and CPTES were reacted under ultrasonic irradiation for 1 h in water. The formation of [*N*′-(3-triethoxysilanepropyl) guanidino]acetic acid **3** that was the only product of the mentioned reaction was identified using ^{1}H NMR (Scheme 2). GA/Fe_3O_4@SiO_2 was produced by grafting of **3** onto the surface of Fe_3O_4@SiO_2, which supports the proposed catalyst structure (Scheme 2, pathway 2). Cu/GA/CPTES was prepared by the chelation of copper by GA/CPTES in water as solution (pathway 3).

FT-IR spectroscopy was used to identify the incorporation of GA-based dendrimers on the silica surface. The FT-IR spectra for modified Fe_3O_4@SiO_2, GA/Fe_3O_4@SiO_2 and Cu/GA/Fe_3O_4@SiO_2 are shown in Fig. 1. The broad band at 580 cm^{-1} is characteristic of stretching vibration of Fe–O–Fe, characteristic of magnetite Fe_3O_4, and the peak at 1635 cm^{-1} can be assigned to the OH deformation of water molecules adsorbed on the materials The typical Si–O–Si bands at 453, 792 and 1085 cm^{-1} present in the spectra of all samples are attributed to the condensed silica network. The strong absorption band at about 3425 cm^{-1} (Figs 1(b) and (c)) is attributed to the OH stretching vibrations of silanol groups. The stretching bands at 2880 and 2945 cm^{-1} are attributed to asymmetric and symmetric C–H stretching in the propyl chain.[31] The GA exists as a zwitterion on the surface of NCPs. This is demonstrated by the existence of the $\delta(NH_3^+)$ band at 2070 cm^{-1}. The lack of this band in the spectra of the complexes shows the copper coordination by the amine terminal group of the GA ligand. Also, two vibrations for the COO– moiety (ν_{as}(COO–) at 1550 cm^{-1} and ν_s(COO–) at 1413 cm^{-1}) are observed in the zwitterion. After coordination there is a lowering of the frequency of one of these bands, due to the generation of the Cu–O bond, and an increase of the other, because a C=O double bond is partially reconstructed. In our complexes, ν_s (COO–) shifts to low frequencies (1389–1397 cm^{-1}) and ν_{as}(COO–) is at 1485 cm^{-1}. For GA/Fe_3O_4@SiO_2 and Cu/GA/Fe_3O_4@SiO_2, the C=N stretching peak of GA overlaps with the broader and stronger bands of Si–O–Si.[32] These results confirm the successful functionalization of NCPs with GA and Cu-chelating GA groups on NCPs.

The crystalline structure of magnetite nanoparticles (before and after silica coating) was identified with the XRD technique. Figure 2

shows the XRD patterns of Fe_3O_4, $Fe_3O_4@SiO_2$, modified $Fe_3O_4@SiO_2$, $GA/Fe_3O_4@SiO_2$ and $Cu/GA/Fe_3O_4@SiO_2$. For Fe_3O_4, diffraction peaks at various angles (2θ) are attributed to the corresponding planes of cubic spinel Fe_3O_4, and are in good agreement with the reported XRD patterns of Fe_3O_4 NCPs.[33] The silica-coating process and further functionalization with CPTES and GA, and immobilization of Cu(II) do not influence the crystalline structure of the Fe_3O_4 core. Therefore, XRD patterns similar to that of Fe_3O_4 are also observed for all steps. The (311) XRD peak was used to determine the mean nanoparticle diameter using Scherrer's equation, $D = 0.9\lambda/(\beta \cos\theta)$, where D is the average crystalline size, λ is the wavelength (Cu Kα, 1.54 Å), β is the angular line width of half-maximum intensity (full width at half maximum) and θ is the Bragg diffraction angle in degrees.[34] The mean crystallite size is calculated as 10 nm.

Figure 3 shows TEM and SEM images of magnetic silica NCPs. As shown in these images, prepared core–shell particles are fairly uniform in shape and size. The size of particles is in the range 80–90 nm with an average size of 10 nm of the magnetic core and an average thickness of the silica shell of 10–15 nm was measured from these images. This size uniformity of the core–shell particles arises from the formation of uniformly sized magnetite cluster cores and follows a uniform covering with the silica shells. These images reveal that the modified magnetic silica NCPs, $GA/Fe_3O_4@SiO_2$ and $Cu/GA/Fe_3O_4@SiO_2$ are similar in size (70–80 nm) and are spherical in shape with highly dispersed particles (Figs 3(a)–(e)). The SEM images of $Cu/GA/Fe_3O_4@SiO_2$ in Figs 3(f) and (g) show the granular and spherical morphology for these NCPs. The average size of 70–85 nm obtained from SEM analysis is compatible with the TEM results.

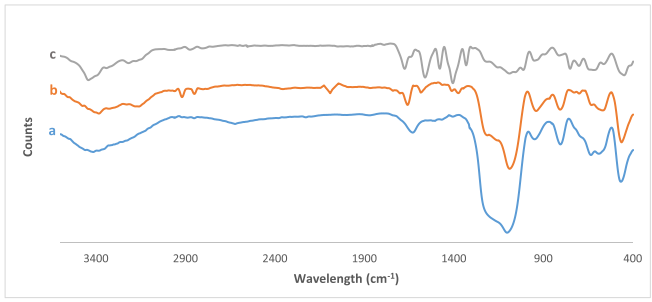

Figure 1. FT-IR spectra of (a) modified $Fe_3O_4@SiO_2$, (b) $GA/Fe_3O_4@SiO_2$ and (c) $Cu/GA/Fe_3O_4@SiO_2$.

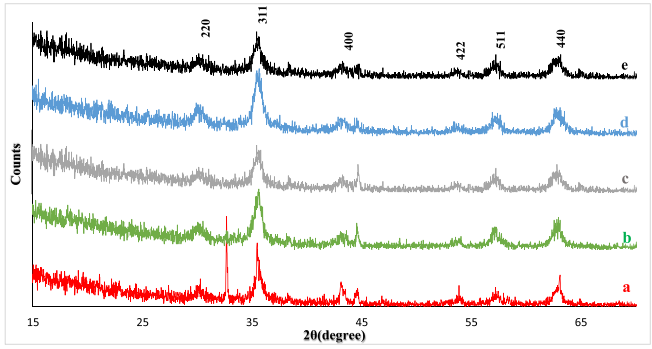

Figure 2. XRD patterns of (a) Fe_3O_4, (b) $Fe_3O_4@SiO_2$, (c) modified $Fe_3O_4@SiO_2$, (d) $GA/Fe_3O_4@SiO_2$ and (e) $Cu/GA/Fe_3O_4@SiO_2$.

From the elemental analysis (CHN) results in Table 1, it is observed that there is an increase in carbon content and also in hydrogen and nitrogen content after functionalization of the modified $Fe_3O_4@SiO_2$ with GA. This indicates the successful attachment of organic fragments (GA) onto the surface of the modified NCPs. Also, the elemental analysis of $Cu/GA/Fe_3O_4@SiO_2$ shows a decrease in content of these elements, because the inorganic content of nanoparticles increases after immobilization of Cu on surface. Furthermore, the presence of Cu in $Cu/GA/Fe_3O_4@SiO_2$ nanocatalyst is confirmed from EDX analysis, indicating the presence of Cu, Si, O, Fe, C and N (Fig. 4). The peaks corresponding to C and N are originated by GA-functionalized NCPs. The contents of these elements for $Cu/GA/Fe_3O_4@SiO_2$ nanocatalyst are given in Table 2. The peaks derive from the copper grid used in SEM measurements.

TGA curves of modified $Fe_3O_4@SiO_2$, $GA/Fe_3O_4@SiO_2$ and $Cu/GA/Fe_3O_4@SiO_2$ NCPs are presented in Fig. 5. The initial weight losses below 150°C are related to the adsorbed moisture in the samples. The decomposition that starts at *ca* 415°C, and continues until *ca*

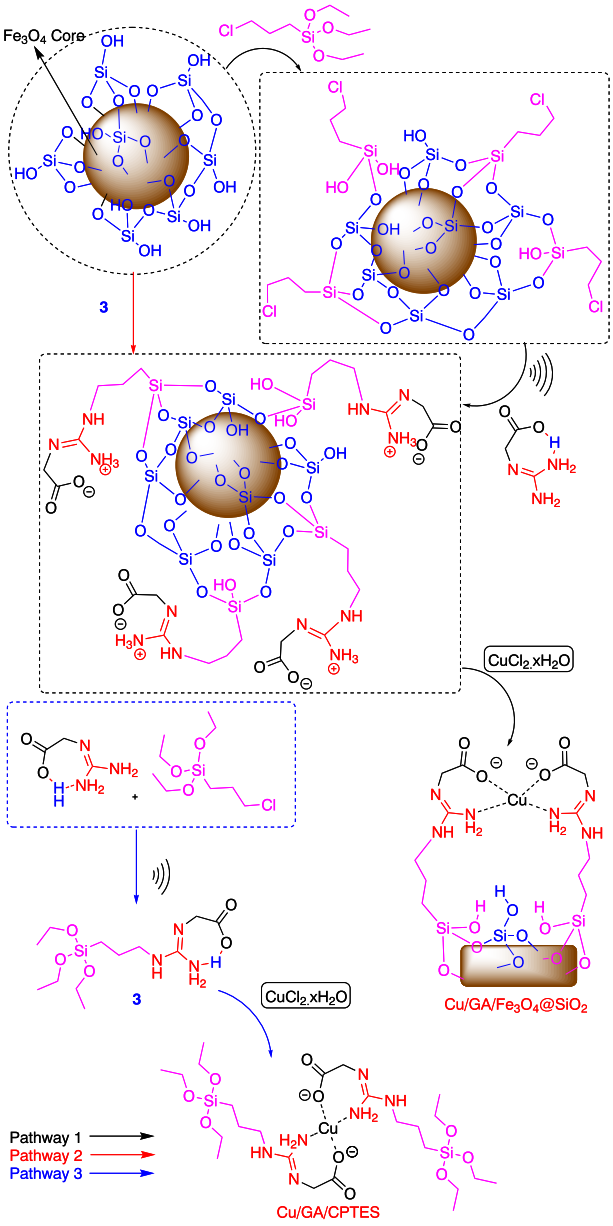

Scheme 2. Pathways for preparation of heterogeneous and homogeneous catalysts.

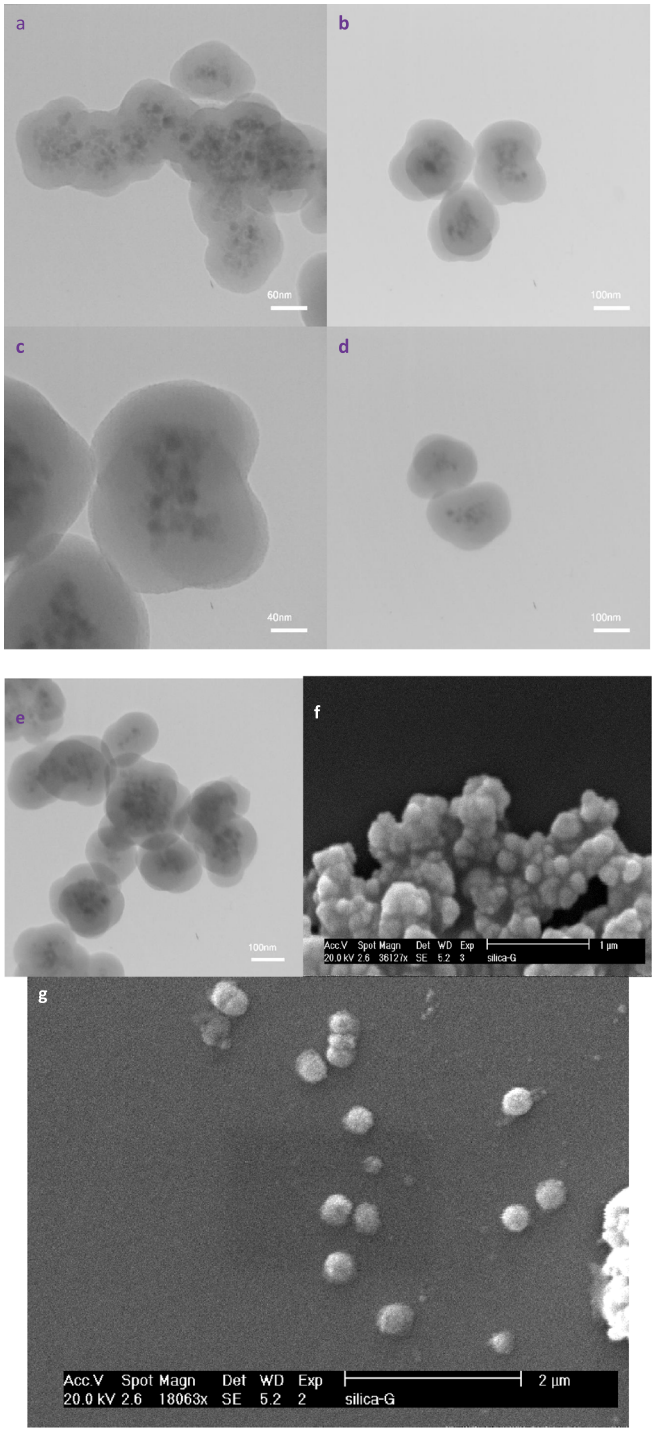

Figure 3. TEM images of (a) modified Fe_3O_4@SiO_2, (b, c) GA/Fe_3O_4@SiO_2 and (d, e) Cu/GA/Fe_3O_4@SiO_2. (f, g) SEM images of Cu/GA/Fe_3O_4@SiO_2.

Table 1. Elemental analysis (CHN) results

Element (mg g^{-1})	Modified Fe_3O_4@SiO_2	GA/ Fe_3O_4@SiO_2	Cu/GA/ Fe_3O_4@SiO_2
N	0	6.724	5.652
C	30.232	37.517	35.914
H	2.071	4.741	3.884

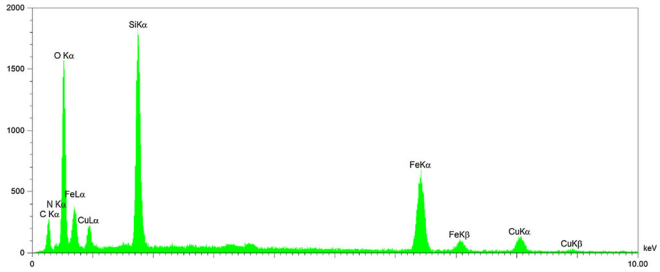

Figure 4. EDX analysis of Cu/GA/Fe_3O_4@SiO_2 NCPs.

Table 2. EDX analysis data for Cu/GA/Fe_3O_4@SiO_2 NCPs

Element	C	N	O	Si	Fe	Cu	Total
Weight (%)	3.61	1.58	12.96	10.12	68.91	2.93	100.00

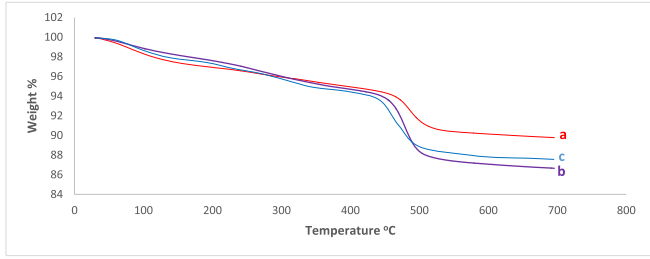

Figure 5. TGA analysis of (a) modified Fe_3O_4@SiO_2, (b) GA/Fe_3O_4@SiO_2 and (c) Cu/GA/Fe_3O_4@SiO_2.

540°C, is associated with the decomposition of the organic chains. The organic species decompose completely at temperatures higher than 600°C and the residual weights of modified Fe_3O_4@SiO_2, GA/Fe_3O_4@SiO_2 and Cu/GA/Fe_3O_4@SiO_2 are 90 and 86 and 88%, respectively, at 700°C. In other words, the results demonstrate percentages of 4, 9 and 7% for organic groups on the surface of modified Fe_3O_4@SiO_2, GA/Fe_3O_4@SiO_2 and Cu/GA/Fe_3O_4@SiO_2, respectively. The differences between modified Fe_3O_4@SiO_2 and GA/Fe_3O_4@SiO_2 confirm the successful immobilization of GA on the surface of modified Fe_3O_4@SiO_2 NCPs. Also, GA/Fe_3O_4@SiO_2 and Cu/GA/Fe_3O_4@SiO_2 exhibit a slight weight loss in the temperature range 200–300°C that can be related to the partial degradation of GA. This phenomenon is not observed for modified Fe_3O_4@SiO_2. The TGA curve of Cu/GA/Fe_3O_4@SiO_2 shows a decrease in loss of weight because the inorganic content of NCPs increases after chelation of Cu on the surface of GA/Fe_3O_4@SiO_2.

The magnetization loop related to Cu/GA/Fe_3O_4@SiO_2 NCPs at room temperature is presented in Fig. 6. As can be seen, resultant particles remain superparamagnetic since there is a minimal coercivity value and remanence on the magnetization loop. The M_s value for the core–shell particles (36 emu g^{-1}) is determined to be significantly lower than that of Fe_3O_4 nanoparticles (62 emu g^{-1}) as a result of the presence of the diamagnetic silica shells surrounding the magnetic cores.[35] It is worth mentioning that the M_s value of the prepared core–shell nanocomposite material is much larger

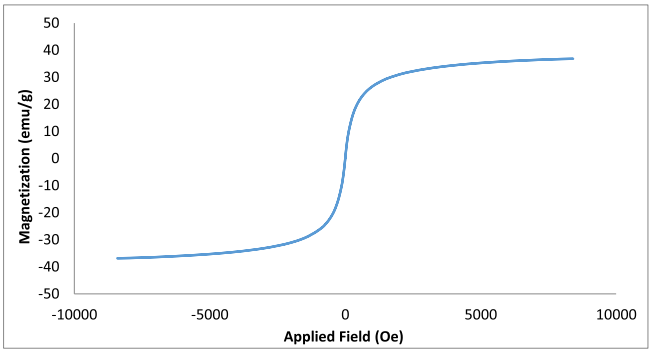

Figure 6. Magnetization loop of Cu/GA/Fe_3O_4@SiO_2 nanoparticles.

Table 3. Optimization of reaction conditions[a] for synthesis of substituted benzodiazepine derivative **1a**

Entry	Catalyst	Grams of catalyst (mol%)	Solvent	Temperature (°C)	Yield (%)[b]
1	Cu/GA/Fe_3O_4@SiO_2	0.010 (0.72)	Water	90	Trace
2	Cu/GA/Fe_3O_4@SiO_2	0.010 (0.72)	Neat	90	60
3	Cu/GA/Fe_3O_4@SiO_2	0.010 (0.72)	EtOH	60	99
4	Cu/GA/Fe_3O_4@SiO_2	0.010 (0.72)	EtOH	r.t.	30
5	Cu/GA/Fe_3O_4@SiO_2	0.007 (0.50)	EtOH	60	67
6	$CuCl_2$	0.007 (5)	EtOH	60	35
7	$CuCl_2$	0.007 (5)	Neat	90	25
8	Fe_3O_4	0.030	EtOH	60	32
9	Fe_3O_4@SiO_2	0.040	EtOH	60	29
10	GA/Fe_3O_4@SiO_2	0.040	EtOH	60	36
11	Cu/GA/CPTES	0.020 (3)	EtOH	r.t.	Trace
12	Cu/GA/CPTES	0.020 (3)	EtOH	60	50
13	Cu/GA/CPTES	0.020 (3)	Neat	90	43

[a] *o*-Phenylenediamine (1 mmol), dimedone (1 mmol) and 4-nitrobenzaldehyde (1 mmol) in the presence of catalyst in solvent.
[b] Isolated yield.

than that of previously published reports.[35,36] This is due to the formation of magnetite cluster cores.

Evaluation of catalytic activity of Cu/GA/Fe_3O_4@SiO_2 in synthesis of substituted benzodiazepine and imidazole derivatives

In order to investigate the catalytic activity of Cu/GA/Fe_3O_4@SiO_2 in the synthesis of substituted benzodiazepines, the one-pot three-component condensation reaction of *o*-phenylenediamine, dimedone and 4-nitrobenzaldehyde was carried out under various reaction conditions. The reaction was examined in solvents such as water and EtOH and under solvent-free conditions. In the case of EtOH, the best performance of the nanocatalyst is observed. Next, the reaction was conducted at ambient temperature and 60°C to obtain the optimum temperature of the reaction in EtOH. This reaction was repeated in the presence of various catalysts such as $CuCl_2$, Fe_3O_4, Fe_3O_4@SiO_2, GA/Fe_3O_4@SiO_2 and Cu/GA/CPTES. The results show that Cu/GA/Fe_3O_4@SiO_2 is more suitable for this reaction. Finally, it is found that using 0.01 g of

Table 5. Optimization of reaction conditions[a] for synthesis of substituted imidazole **2a**

Entry	Catalyst	Grams of catalyst (mol%)	Temperature (°C)	Yield (%)[b]
1	Cu/GA/Fe_3O_4@SiO_2	0.010 (0.72)	r.t.	30
2	Cu/GA/Fe_3O_4@SiO_2	0.010 (0.72)	90	92
3	Cu/GA/Fe_3O_4@SiO_2	0.020 (1.44)	90	92
4	$CuCl_2$	0.007 (5)	90	25
5	Fe_3O_4	0.030	90	30
6	Fe_3O_4@SiO_2	0.040	90	Trace
7	GA/Fe_3O_4@SiO_2	0.040	90	38
8	Cu/GA/CPTES	0.020 (3)	r.t.	Trace
9	Cu/GA/CPTES	0.020 (3)	90	50

[a] Benzil (1 mmol), benzaldehyde (1 mmol) and ammonium acetate (1 mmol) in the presence of catalyst under solvent-free conditions for 60 min.
[b] Isolated yield.

Table 4. Synthesis of 1,5-benzodiazepines.

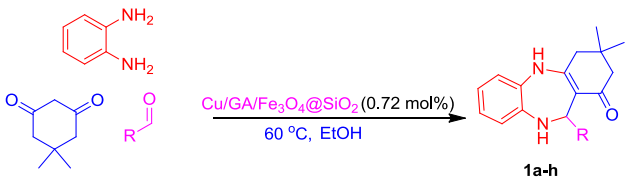

1a-h

Entry	R	Product	Yield (%)	$m.p._{rep}/m.p._{lit}$ (°C)
1	4-Nitrobenzaldehyde	**1a**	99	272–273/274–275[17]
2	4-Chlorobenzaldehyde	**1b**	95	236–238/235–237[16]
3	2-Hydroxybenzaldehyde	**1c**	88	159–161/158–159[16]
4	2,4-Dichlorobenzaldehyde	**1d**	96	248–250/246–249[18]
5	3-Nitrobenzaldehyde	**1e**	90	148–150/147–148[18]
6	4-Methylbenzaldehyde	**1f**	90	130–135/134–136[17]
7	Furan-2-carbaldehyde	**1 g**	94	215–218/216–218[16]
8	Pyridine-2-carbaldehyde	**1 h**	90	233–235/230–232[17]

Cu/GA/Fe_3O_4@SiO_2 in EtOH at 60°C is sufficient to push the reaction forward (Table 3).

Syntheses of 1,5-benzodiazepine derivatives **1a**–**h** with various aromatic and heteroaromatic aldehydes under optimum conditions were conducted. As evident from Table 4, all reactions occur successfully in high to excellent yields for relatively short reaction times. This reaction with aldehydes containing electron-withdrawing R groups is accomplished in excellent yields.

In addition, the efficiency of catalysts Cu/GA/Fe_3O_4@SiO_2, $CuCl_2$, Fe_3O_4, Fe_3O_4@SiO_2, GA/Fe_3O_4@SiO_2 and Cu/GA/CPTES was examined for the synthesis of 2,4,5-trisubstituted imidazoles via reaction of benzil, benzaldehyde and ammonium acetate under solvent-free conditions. The best reaction conditions include use of 0.01 g of Cu/GA/Fe_3O_4@SiO_2 at 90°C (Table 5, entry 2). As indicated in Table 5 (entries 4–9), the reaction yields are less in the presence of $CuCl_2$, Fe_3O_4, Fe_3O_4@SiO_2, GA/Fe_3O_4@SiO_2 and Cu/GA/CPTES.

Subsequently, to investigate the efficiency and applicability of this catalyst in the three-component synthesis of 2,4,5-trisubstituted 1 *H*-imidazoles **2a**–**h**, the reaction was extended to other substituted benzaldehydes using optimum catalyst amount and temperature under solvent-free conditions. High yields are obtained using both electron-donating and electron-withdrawing groups (Table 6).

Recyclability of Cu/GA/Fe_3O_4@SiO_2 was examined in both of the syntheses discussed above. The recycling was carried out by applying an external magnet to the reaction vessel. Separation of the nanocatalyst particles is achieved within seconds and the supernatant containing the product can be decanted. The catalyst was reused in the reaction after washing with EtOH and drying under vacuum at 90°C for 3 h. This procedure was carried out for five repeat cycles. The results show that only minor decreases in the reaction yields are observed (Fig. 7).

Catalyst stability

Comparison between the FT-IR results (Fig. 8) and CHN and ICP-OES results (Table 7) for the as-prepared (fresh) catalyst and the reused catalyst demonstrates the high stability of the catalyst in both of the syntheses discussed above, without significant change in content of Cu, C, N and H.

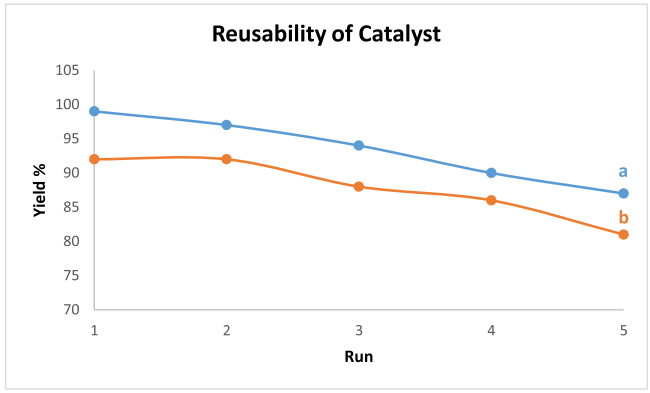

Figure 7. Recyclability of Cu/GA/Fe_3O_4@SiO_2 in the synthesis of (a) benzodiazepines and (b) imidazoles. (c) Dispersion of Cu/GA/Fe_3O_4@SiO_2 particles. (d) Recycling of the catalyst through magnetic decantation.

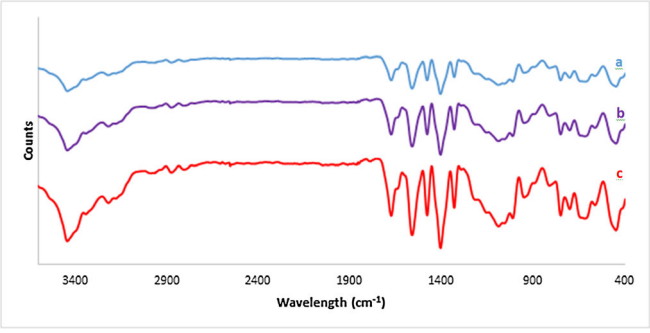

Figure 8. FT-IR spectra of (a) as-prepared Cu/GA/Fe_3O_4@SiO_2, (b) Cu/GA/Fe_3O_4@SiO_2 after fifth run in the synthesis of benzodiazepines and (c) Cu/GA/Fe_3O_4@SiO_2 after fifth run in the synthesis of imidazoles.

Table 6. Synthesis of trisubstituted imidazoles.

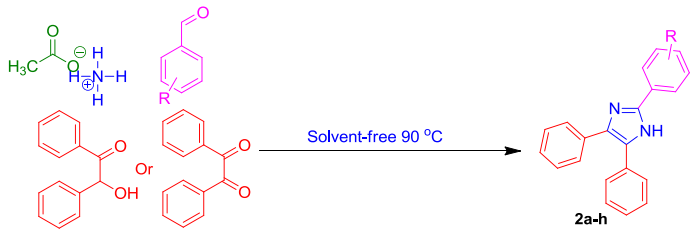

Entry	R	Product	Benzil/benzoin yield (%)	$m.p._{rep}/m.p._{lit}$[19] (°C)
1	H	**2a**	92/90	270–273/270–272
2	4-Cl	**2b**	96/90	258–261/256–258
3	4-Br	**2c**	96/91	259–262/259–261
4	4-CH_3	**2d**	90/90	228–230/227–229
5	4-OCH_3	**2e**	92/90	230–235/231–233
6	4-NO_2	**2f**	98/95	196–198/194–196
7	3-NO_2	**2 g**	95/94	292–294/290–292
8	2,4-Cl	**2 h**	97/92	165–168/168–170

Table 7. Elemental analysis (CHN and ICP-OES) results for reused Cu/GA/Fe_3O_4@SiO_2

Element	As-prepared	After five uses[a]	After five uses[b]
N (mg g^{-1})	5.652	5.719	5.524
C (mg g^{-1})	35.914	36.017	35.225
H (mg g^{-1})	3.884	3.941	3.512
Cu (mmol g^{-1})[c]	0.720	0.690	0.710

[a] Cu/GA/Fe_3O_4@SiO_2 after fifth run in the synthesis of benzodiazepines.
[b] Cu/GA/Fe_3O_4@SiO_2 after fifth run in the synthesis of imidazoles.
[c] ICP-OES data.

Conclusions

A highly efficient Cu(II) nanocatalyst based on functionalized magnetic silica NCPs, Cu/GA/Fe_3O_4@SiO_2, has been synthesized. Characterization results of these NCPs show that the catalyst provides highly disperse nanoparticles with a high thermal stability. According to these properties, its catalytic application was evaluated in the synthesis of benzodiazepine and imidazole derivatives in EtOH and under solvent-free conditions, respectively. The results show that the nanocatalyst is effective, recoverable and stable under the reaction conditions.

Acknowledgments

We gratefully acknowledge financial support from the Research Council and Catalyst Center of Excellence (CCE) of Shahid Beheshti University and Iran National Elites Foundation (INEF).

References

[1] C. R. Martin, P. Kohli, *Nat. Rev. Drug Discov.* **2003**, *2*, 29–37.
[2] M. C. Roco, *Curr. Opin. Biotechnol.* **2003**, *14*, 337–46.
[3] D. J. de Aberasturi, A. B. Serrano-Montes, L. M. Liz-Marzán, *Adv. Opt. Mater.* **2015**, *3*, 602–17.
[4] H. Ding, Y. Zhang, S. Wang, J. M. Xu, S. C. Xu, G. H. Li, *Chem. Mater.* **2012**, *24*, 4572–80.
[5] S. Laurent, D. Forge, M. Port, A. Roch, C. Robic, L. V. Elst, R. N. Muller, *Chem. Rev.* **2008**, *108*, 2064–110.
[6] N. R. Shiju, V. V. Guliants, *Appl. Catal. A* **2009**, *356*, 1–17.
[7] R. S. K. Singh, B. Kashyap, P. Phukan, *Tetrahedron Lett.* **2013**, *54*, 6687–90.
[8] R. N. Baig, R. S. Varma, *Chem. Commun.* **2013**, *49*, 752–70.
[9] B. B. Toure, D. G. Hall, *Chem. Rev.* **2009**, *109*, 4439–86.
[10] A. Domling, W. Wang, K. Wang, *Chem. Rev.* **2012**, *112*, 3083–135.
[11] A. Z. Halimehjani, I. N. Namboothiri, S. E. Hooshmand, *RSC Adv.* **2014**, *4*, 48022–84.
[12] R. Grigg, *Chem. Soc. Rev.* **1987**, *16*, 89–121.
[13] B. Ganem, *Acc. Chem. Res.* **2009**, *42*, 463–72.
[14] R. Tannert, A. Moran, P. Melchiorre, in *Comprehensive Enantioselective Organocatalysis: Catalysts, Reactions, and Applications*, Wiley-VCH, Weinheim, **2013**, pp. 1285–1331.
[15] M. Curini, F. Epifano, M. C. Marcotullio, O. Rosati, *Tetrahedron Lett.* **2001**, *42*, 3193–5.
[16] A. Sabatié, D. Végh, A. Loupy, L. Floch, *ARKIVOC* **2001**, *6*, 122–8.
[17] R. K. Sharma, S. Gulati, A. Pandey, *Inorg. Chim. Acta* **2013**, *397*, 21–31.
[18] A. Maleki, M. Kamalzare, *Tetrahedron Lett.* **2014**, *55*, 6931–4.
[19] A. Shaabani, A. Rahmati, E. Farhangi, Z. Badri, *Catal. Commun.* **2007**, *8*, 1149–52.
[20] G. V. M. Sharma, Y. Jyothi, P. S. Lakshmi, *Synth. Commun.* **2006**, *36*, 2991–3000.
[21] M. M. Heravi, M. Daraie, V. Zadsirjan, *Mol. Divers.* **2015**, 1–47.
[22] N. Kolos, E. Yurchenko, V. Orlov, S. V. Shishkina, O. V. Shishkin, *Chem. Heterocycl. Compd.* **2004**, *40*, 1550–9.
[23] Y. Wang, M.-S. Tu, F. Shi, S.-J. Tu, *Adv. Synth. Catal.* **2014**, *356*, 2009–19.
[24] D. V. Jarikote, S. A. Siddiqui, R. Rajagopal, T. Daniel, R. J. Lahoti, K. V. Srinivasan, *Tetrahedron Lett.* **2003**, *44*, 1835–8.
[25] P. Salehi, M. Dabiri, M. A. Zolfigol, S. Otokesh, M. Baghbanzadeh, *Tetrahedron Lett.* **2006**, *47*, 2557–60.
[26] M. Dabiri, P. Salehi, M. Baghbanzadeh, M. S. Nikcheh, *Synth. Commun.* **2008**, *38*, 4272–6.
[27] A. Shaabani, A. H. Rezayan, S. Keshipour, A. Sarvary, S. W. Ng, *Org. Lett.* **2009**, *11*, 3342–5.
[28] M. Mahyari, M. S. Laeini, A. Shaabani, *Chem. Commun.* **2014**, *50*, 7855–7.
[29] A. Shaabani, A. Maleki, F. Hajishaabanha, H. Mofakham, M. Seyyedhamzeh, M. Mahyari, S. W. Ng, *J. Comb. Chem.* **2010**, *12*, 186–90.
[30] R. K. Iller, *The Chemistry of Silica*, John Wiley, New York, **1979**.
[31] S. Ahmad, U. Riaz, A. Kaushik, J. Alam, *J. Inorg. Organometal. Polym.* **2009**, *19*, 355–60.
[32] M. Jafarzadeh, E. Soleimani, H. Sepahvand, R. Adnan, *RSC Adv.* **2015**, *5*, 42744–53.
[33] C. Hui, C. Shen, J. Tian, L. Bao, H. Ding, C. Li, Y. Tian, X. Shi, H.-J. Gao, *Nanoscale* **2011**, *3*, 701–5.
[34] P. Scherrer, *Gött. Nachricht. Gesell.* **1918**, *2*, 98–100.
[35] M. Kalantari, M. Kazemeini, A. Arpanaei, *Mater. Res. Bull.* **2013**, *48*, 2023–8.
[36] C. Vogt, M. S. Toprak, M. Muhammed, S. Laurent, J.-L. Bridot, R. N. Müller, *J. Nanoparticle Res.* **2010**, *12*, 1137–47.